INTERNATIONAL JOURNAL OF HYDROGEN ENERGY 43 (2018) 667–675

Available online at www.sciencedirect.com

ScienceDirect

journal homepage: www.elsevier.com/locate/he

Analysis of syngas production rate in empty fruit bunch steam gasification with varying control factors[☆]

Yueh-Heng Li[*], *Hsiang-Ho Chen*

Department of Aeronautics and Astronautics, National Cheng Kung University, Tainan 701, Taiwan, ROC

ARTICLE INFO

Article history:
Received 17 July 2017
Received in revised form
12 November 2017
Accepted 19 November 2017
Available online 9 December 2017

Keywords:
Steam gasification
Palm
Empty fruit bunch
Torrefaction
Syngas

ABSTRACT

Biomass gasification is a prevailing approach for mitigating irreversible fossil fuel depletion. In this study, palm empty fruit bunch (EFB) was steam-gasified in a fixed-bed, batch-fed gasifier, and the effect of four control factors—namely torrefaction temperature for EFB pretreatment, gasification temperature, carrier-gas flow rate, and steam flow rate—on syngas production were investigated. The results showed that steam flow rate is the least influential control factor, with no effect on syngas composition or yield. The gasification temperature of biomass significantly affects the composition of syngas generated during steam gasification, and the H_2/CO ratio increases by approximately 50% with an increase in temperature ranging from 680 °C to 780 °C. The higher H_2/CO ratio at a lower gasification temperature increased the energy density of the combustible constituents of the syngas by 3.43%.

Introduction

Fossil fuel depletion is primarily attributed to the enormous energy demand of modern civilization, which has resulted in excessive carbon dioxide emission and unprecedented global warming. Many attempts have been made to avert global warming crises through the increased use of renewable energy, such as solar, wind, and geothermal energy. However, almost all renewable energy sources have drawbacks associated with their intermittent power output, which is dependent on the weather and season, and their topographical limitations regarding construction site. By contrast, biomass is a cheap and abundant source of energy that has good synergy with current fossil fuel power plants. With the objective of mitigating carbon dioxide emission, several research groups have examined the possibility of using biomass to replace at least a portion of current fossil fuel consumption [1].

The direct burning of biomass has several disadvantages, such as low heating value, high moisture content, corrosion problems, wide particle-size distribution, and low homogeneity [2]. To improve the fuel properties of biomass, many thermochemical and biological process are applied to obtain high-quality fuels from biomass. One of these, gasification is a high-temperature process wherein organic and fossil fuel-based carbonaceous materials are converted into carbon

---

[☆] This manuscript is submitted for publication in ***International Journal of Hydrogen Energy*** and has neither been published in nor submitted to a journal previously, nor will it be submitted to another journal during the ***Int'l J. of Hydrogen Energy*** review process.

[*] *Corresponding author.*
E-mail address: yueheng@mail.ncku.edu.tw (Y.-H. Li).

https://doi.org/10.1016/j.ijhydene.2017.11.117

monoxide, hydrogen, and carbon dioxide with assistance from a gasifying agent. Moisture in the biomass is gradually discharged as the ambient temperature increases to 100 °C, resulting in 5–10% weight loss depending on the type of biomass feedstock [3,4]. As the temperature further increases to 250–400 °C, large carbohydrate compounds, such as starch, hemicellulose, and cellulose, decompose into smaller molecules (e.g., carbon dioxide, methane, acetic acid, and phenol), resulting in major mass loss (approximately 40%). The solid reaction product (char) mostly comprises carbon. Finally, gasification occurs at a high temperature of approximately 650 °C, with the gasifying agents (typically air, because of its low cost) initiating the reaction with carbon in the char and releasing gaseous compounds.

Table 1 presents a list of the major reactions that occur during gasification. The solid residue, called ash, mainly comprises metal oxides. Using oxygen and steam as the gasification agents is expensive and necessitates a complicated gasifier design; however, they produce reaction products with higher heating values than does air. Syngas—which mainly comprises hydrogen and carbon monoxide, with relatively small amounts of methane, carbon dioxide, and other gaseous hydrocarbons such as ethane—is the combustible gas mixture resulting from gasification. The composition of syngas depends on many gasification parameters, such as biomass type, gasification agent, and temperature. Syngas can be used as fuel in internal combustion engines and fuel cells. Biomass gasification can therefore reduce greenhouse gas emission because syngas can partially replace fossil fuels in, for example, hydrogen production [5].

Torrefaction alters the physical and chemical properties of biomass. Torrefied biomass has a relatively higher heating value and lower weight, and is hydrophobic [8]. Torrefaction can thus be considered a means to upgrade the quality of solid biomass, or as pretreatment for gasification. For example, Chew and Doshi [9] reported that a reduction of tar precursors such as acetol and guaiacol was observed after torrefaction of pine. Additionally, they mentioned that torrefaction improved the reactivity of biofuel, thus reducing the required gasifier size. Similarly, other researchers have also reported on enhancing gasification through torrefaction as pretreatment. Deng et al. [10] reported the beneficial effects of co-gasification of coal and torrefied biomass and recommended that small pretreatment factories for torrefaction be built near biomass resources to conveniently obtain high-energy-content char or gas; this gas can subsequently be gasified on a large scale far away from the farmland. Apart from preventing the use of raw biomass, other benefits of torrefaction include simplified milling and enhanced gasifier efficiency due to biomass moisture reduction. Prins et al. [11] reported that pretreating biomass through torrefaction increases the gasification efficiency (exergy balance). Couhert et al. [12] confirmed that pretreating biomass through torrefaction increased the amount of CO and H_2 in gaseous gasification products.

Table 1 – Main gasification reactions [6,7].

Chemical reaction	Kinetics scheme
Boudouard	$C(s) + CO_2 \rightleftharpoons 2CO$
Water–gas (Heterogeneous)	$C(s) + H_2O \rightleftharpoons CO + H_2$
Hydrogenation	$C(s) + 2H_2 \rightleftharpoons CH_4$
Partial oxidation	$2C(s) + O_2 \rightleftharpoons 2CO$
WGS	$CO + H_2O \rightleftharpoons CO_2 + H_2$
Methane reforming (steam)	$CH_4 + H_2O \rightleftharpoons CO + 3H_2$

The use of a gasification agent is another factor that strongly influences gasification. The gasification agent reacts with biomass and breaks it down into gas molecules (notably, the biomass also breaks down under high temperatures through, for example, pyrolysis). Of the many gasification agents, air is the most common; although its oxygen content is only 21%, air is abundant and requires no storage equipment. Pure oxygen can also be used as a gasification agent to increase the heating values of syngas. Once the reaction is initiated, these two gasification agents achieve self-sufficiency, meaning that no external energy is needed. Steam is another agent used for its ability to extract the most amount of hydrogen from biomass; however, it requires additional power input [7]. Occasionally, CO_2 is used as the gasification agent to enhance CO_2 recycling and to reduce CO_2 concentration in the atmosphere.

Several control factors, such as the amount of gasification agent, biomass characteristics, and gasification temperature, affect the outcome of gasification. The effects of these control factors on the products of steam gasification have been extensively investigated. For example, Salmiaton et al. [13] studied the effect of air flow rate, particle size, and gasification temperature on the composition and yield of syngas and reported that a high gasification temperature considerably increased both the yield and heating value of syngas. This increase in heating value is due to the lower CO_2 composition in the syngas at high temperatures. In addition, a smaller particle size slightly increased the syngas production, and an increase in air flow increased the syngas yield but decreased the heating value. Guan et al. [14] examined the effects of biomass type, temperature, and steam flow rate, and found that wood (which is mostly composed of cellulose and lignin) was harder to gasify than was seaweed and that mixing seaweed with wood promoted the gasification reaction of wood. Moreover, introducing a steam flow increased syngas yield, but excessive steam flow decreased the yield because a large steam flow cools the reactor [15]. As was the case in air gasification, a high temperature in steam gasification increased syngas yield.

Many studies have also focused on the time evolution of syngas production. Moon et al. [16] classified the gasification reaction into two, often overlapping, stages: devolatilization and char gasification. In the devolatilization stage, the reaction is limited by the rates of heat transfer and molecule diffusion. Thermodecomposing biomass rapidly produces volatility. In the char reaction stage, the reaction progresses relatively slowly. Overall, Moon et al. reported that high temperatures and steam flow rates promote both devolatilization and char reaction. Wood et al. [17] examined the influence of biomass composition on the gasification of several types of biochar. All biochars exhibited similar two-stage reaction characteristics, and the syngas production time curve varied with the microstructural and elemental composition of the biomasses.

Empty fruit bunch (EFB) is the residue created by palm-oil production. EFBs are abundant because palm fruits are a major source of edible oil. Several groups have studied the feasibility of EFBs as an energy source [13,18,19]. Table 2 presents the composition of EFBs. The present study examined the effect of torrefaction pretreatment, gasification temperature, carrier-gas flow rate, and steam flow rate on the different reactions and stages in steam gasification.

Methodology

The experiment was designed through the Taguchi method, which facilitates the efficient analysis of multiple control factors. Orthogonal arrays are an important aspect of the Taguchi method. The choice of orthogonal array dictates the number of factors that can be inspected and the number of experiment runs required. This study investigated four factors, each with three levels (Table 3), by using an L_9 orthogonal array (Table 4), where the suffix "9" indicates that nine experiments must be performed. In the Taguchi method, these experimental results are then transformed to a signal-to-noise (S/N) ratio for ease of data interpretation. The S/N ratio algorithm can be logarithmic or inverse, but the exact equation depends on the optimization objectives; typically, three types of optimization targets are employed: smaller-is-best, nominal-is-best, and larger-is-best, respectively. A larger S/N ratio indicates better results (i.e., the obtained data is closer to the desired value).

Fig. 1 is a schematic of the updraft fixed-bed batch gasification system used in this study. This gasifier can achieve a reactor wall temperature of 800 °C, and the nitrogen flow rate is controlled using a float-type flow meter (Dwyer Instruments). A pressurized air tank is connected to a water tank equipped with a needle valve and a ball valve for flow-rate control and shutoff. Two resistive heating devices are controlled using two separate proportional–integral–derivative temperature controllers. The main body of the gasifier is composed of a quartz tube with an inner diameter 64 mm, wall thickness of 2 mm, and length of 500 mm. The ends of this quartz tube are sealed using two steel caps, with Viton O-rings placed between the quartz tube and steel cap for airtightness. This setup also houses an alumina honeycomb sample holder supported by several steel rods.

Table 2 – EFBs with a diameter of 4 mm and length of 5–20 mm (supplied by China Steel Company).

Proximate analysis	Weight percentage (%)
Moisture	4.088
Volatile	64.951
Fixed carbon	19.485
Ash	11.476
Elemental composition	
C	39.0
H	0.57
O	43.0
N	1.30
S	0.13

Table 3 – Parameters and levels in the experiment.

Parameter	Level 1	Level 2	Level 3
[A]: Torrefaction temperature, °C	Raw biomass	250	300
[B]: Steam flow rate, g/min	1.2	1.75	3.0
[C]: N_2 flow rate, L/min	0.8	1.0	1.2
[D]: Gasifier temperature, °C	680	730	780

Before gasification, 3 g of EFB pellets were subjected to torrefaction under the conditions specified in the L_9 orthogonal array. Torrefaction was performed by feeding 1 L/min of nitrogen into the reactor. The samples were held at the specified torrefaction temperature for 1 h. Subsequently, the torrefied (or raw) pellet was placed onto the aluminum honeycomb sample holder. After ensuring airtightness of the gasifier, nitrogen was flowed to purge the remaining air. Then, the gasifier temperature was increased to the target gasification temperature over 50 min by the resistive heating wire on the reactor wall. On reaching the target temperature, steam was flowed into the gasifier. The heater plate then completely evaporated the liquid water. Biosyngas emission was detected and recorded using an industrial gas analyzer (Vario Plus) at a sampling rate of 1/25 Hz for 10 min.

Results and discussion

Taguchi method

A Taguchi L_9 orthogonal array, which can accommodate four parameters with three levels each, was used for designing the experiments. The nitrogen concentration in the product gas was subtracted from 100%. The raw concentration data was then normalized by the difference to obtain the syngas composition. Table 5 shows the H_2/CO ratios obtained in each experiment. Each experiment was performed three times, and in each, data were recorded as the mean of measurements at 24 data points.

The S/N ratio for each factor was calculated as the hydrogen percentage through larger-is-best optimization (Table 6). Entries in the "$S/N_{max} - S/N_{min}$" row indicate the difference between the maximum and minimum S/N ratio for each factor, which directly correlates with the effect of the corresponding factor; this is because changing the level of a factor that has a high influence on the reaction would cause wide variations in the product property, resulting in a higher difference in the measurements at different levels. From Table 6, it is evident that gasification temperature has the strongest effect on gasification and that the effect of steam flow rate is negligible.

To confirm the results obtained through the Taguchi S/N ratio analysis, a confirmation run was executed. The parameter set with the highest S/N ratio is A1, B3, C3, and D1. The predicted S/N ratio, which corresponds to the highest H_2/CO ratio in syngas, can be calculated using the following equation:

$$\eta_{predicted} = \eta_{A1} + \eta_{B3} + \eta_{C3} + \eta_{D1} - 3\overline{\eta}$$

where η represents the S/N ratio, the subscripts on the right-hand side of the equation are the individual S/N ratios for the

Table 4 – Taguchi L_9 array used in this study.

Exp. Run#	Torrefaction temperature (°C)	Steam flow rate (g/min)	Nitrogen flow rate (L/min)	Gasification temperature (°C)
Run 1	No Torrefaction	1.75	1	680
Run 2	No Torrefaction	1.2	0.8	730
Run 3	No Torrefaction	3	1.2	780
Run 4	250	1.75	0.8	780
Run 5	250	1.2	1.2	680
Run 6	250	3	1	730
Run 7	300	1.75	1.2	730
Run 8	300	1.2	1	780
Run 9	300	3	0.8	680

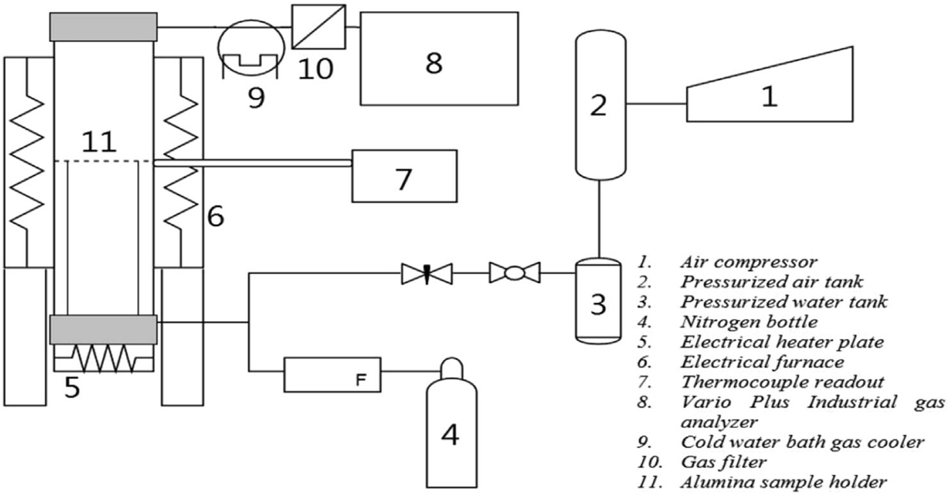

Fig. 1 – Gasifier equipment, cooling system, and gas analyzer used in this study.

Table 5 – H_2/CO ratio for each experiment.

Experiment No.	Run 1	Run 2	Run 3
1	13.40	13.56	13.84
2	8.72	9.62	9.44
3	8.02	9.99	10.41
4	8.35	5.65	6.07
5	12.83	13.89	14.88
6	9.08	9.35	11.16
7	8.98	10.64	9.86
8	6.72	7.24	7.33
9	9.89	10.65	10.70

Table 6 – Effects of the investigated factors.

Level	[A] Torrefaction	[B] Steam	[C] Nitrogen	[D] Temperature
1	**20.44**	19.70	18.60	**21.93**
2	19.57	19.54	19.81	19.62
3	19.04	**19.82**	**20.65**	17.50
$S/N_{max} - S/N_{min}$	1.40	0.28	2.05	4.43

indicated level and parameter, and $\overline{\eta}$ is the average of the nine experimental S/N ratios. The predicted S/N ratio was 23.78, corresponding to a H_2/CO ratio of 15.46 (Table 7). The confirmation run was repeated twice.

Table 7 – Validation of the Taguchi results.

	H_2/CO ratio	S/N ratio
Prediction	15.46	23.78
Confirmation	15.78, 15.43	23.86

Transient analysis

Generally, when biomass is subjected to thermal pretreatment, the majority of residual biomass would be composed of carbon. Consequently, during gasification, the biomass can be theoretically regarded as pure carbon [20]. Typically, gasification reactions include three heterogeneous reactions entailing carbon: the Boudouard reaction, hydrogenating reaction, and steam–carbon (S–C) reaction. Compared with the S–C reaction, the chemical reactivity of the hydrogenating and Boudouard reactions are negligible due to the low value of the reaction rate constant [7]. In addition, CO_2 and H_2 can be considered scarce gases in the gasifier because of their low concentration relative to those of the gasifying agents (i.e., water steam). Thus, the hydrogenating and Boudouard reactions can be ignored in the analysis. Accordingly, the chemical reactions during steam gasification can be simplified to the following three reactions:

$$C + H_2O \rightleftharpoons CO + H_2 \quad \text{Water} - \text{gas (S} - \text{C)} \tag{R1}$$

$$CH_4 + H_2O \rightleftharpoons CO + 3H_2 \quad \text{Methane reforming} \tag{R2}$$

$$CO + H_2O \rightleftharpoons CO_2 + H_2 \quad \text{WGS} \tag{R3}$$

The S–C reaction is a heterogeneous reaction, whereas the methane reforming and WGS reactions are homogeneous reactions. The production rate of the product gases is normalized by dividing the volume fraction of nitrogen. However, because three levels of nitrogen flow rates were employed in the experiment, the average nitrogen flow rate was set at 1 L/min; considering the effect of nitrogen flow rate, all values were multiplied by the following weighting factors: 1.0 for level 1, 0.8 for level 2, and 1.2 for level 3. The effect of each control parameter was obtained by averaging the results of the relevant experiments. For example, the average of experiment runs 1, 5, and 9 represents the effect of a gasification temperature of 680 °C on hydrogen production.

Characteristically, reaction R2 (i.e., methane reforming) is the most efficient among the three reactions. These reactions are reversible, but the forward reactions are extremely strong [6,21]. Methane usually accumulates in the gasifier during the pyrolysis period of gasification. Therefore, the absence of methane during gasification indicates that only the heterogeneous reaction R1 and homogeneous reaction R3 are dominant. In this scenario, the overall product gas would consist of approximately two moles of H_2, one mole of CO_2, and two moles of CO. Inayat et al. [22] reported that the H_2/CO_2 ratio in the absence of sorbent CaO approached 2, where the amount of hydrogen mole fraction was 0.65 and the amount of CO_2 mole fraction was 0.31. In the presence of methane, however, the hydrogen yield would double because of the combined effect of the homogeneous reactions R2 and R3 on hydrogen production. Eventually, the gasification gas constitutes approximately four H_2 molar fractions and one CO_2 molar fraction. Wang et al. [23] posited that in the volatile reaction stage of gasification, the syngas would contain more H_2 than CO and CO_2. Therefore, the H_2/CO_2 ratio can serve as an effective indicator of the competition of volatile reaction (i.e., methane steam reforming) and char reaction (i.e., heterogeneous water–gas reaction) at any given time.

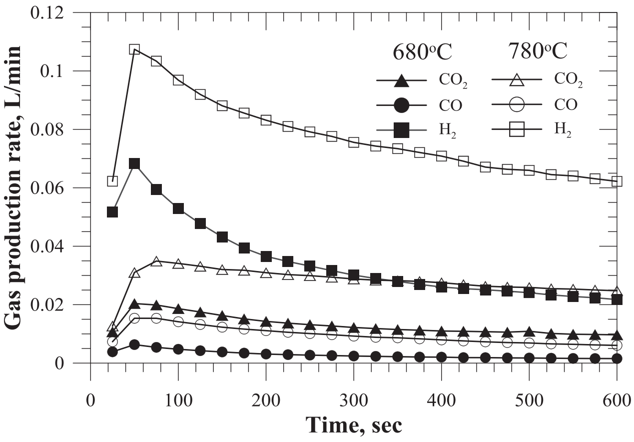

Fig. 2 – Syngas (excluding CH_4) production rate at gasification temperatures of 680 and 780 °C.

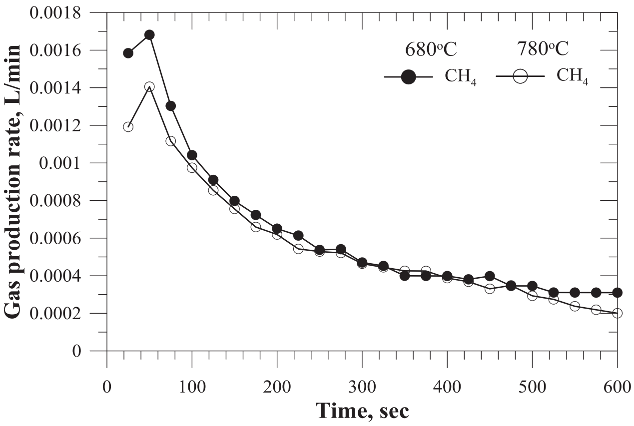

Fig. 3 – Methane production rate at gasification temperatures of 680 and 780 °C.

Effect of gasification temperature

To investigate the effect of gasification temperature on hydrogen yield, the production rates of the main gasification gases, namely H_2, CO, and CO_2, at gasification temperatures of 680 and 780 °C were recorded for 600 s during gasification (Fig. 2). An increase in gasification temperature enhanced the production rate of the main gasification gases. In addition, all measured data had distinct peaks, similar to the case in Moon et al. [16]. These peaks indicate the volatile reaction phase of gasification, whereas the long tails of the gas production curve indicted the slow char phase. However, the two phases do not have a distinct boundary. Fig. 3 shows the methane production rate at various gasification temperatures, which was lower than that of the main gases. By contrast, the methane production rate was low during the volatile reaction during gasification at 780 °C. Nevertheless, the status of the methane reforming reaction can be assessed by monitoring the H_2/CO_2 ratio (Fig. 4). If the methane reforming reaction is activated, R1, R2, and R3 may produce hydrogen, and the H_2/CO_2 ratio becomes equal to or exceeds 4. On the contrary, if the methane reforming reaction is deactivated, hydrogen is primarily produced by R1 and R3, and the H_2/CO_2 ratio approaches 2. As shown in Fig. 4, the H_2/CO_2 ratios at the two investigated gasification temperatures exceeded 4 in the volatile reaction phase because of methane production, and the H_2/CO_2 ratios approached 2 in the char reaction phase. The low methane production rate at 780 °C in Fig. 2 is thus a product of the active methane reforming reaction, which leads to a low methane production rate during the volatile reaction phase.

Furthermore, the competition between the homogeneous WGS reaction and the heterogeneous S–C reaction warrants attention. The WGS reaction (R3) produces equivalent amounts of CO_2 and H_2, whereas the S–C reaction (R1) generates equivalent amounts of CO and H_2. Therefore, the CO_2/CO ratio can be used to determine whether R1 or R3 is dominant: the CO_2/CO ratio is larger than unity when the homogeneous reaction is dominant, and vice versa. Fig. 5 is a plot of

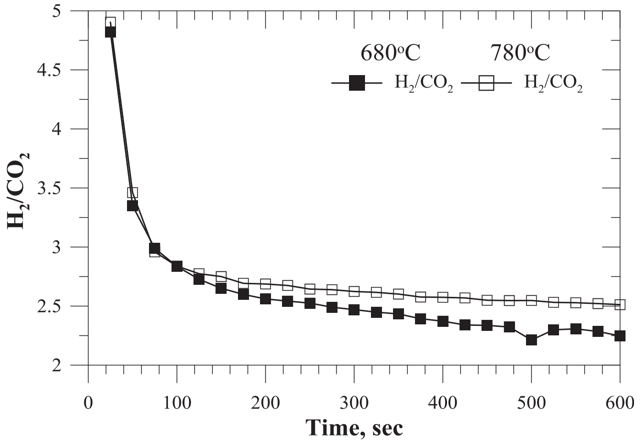

Fig. 4 – H_2/CO_2 ratios at gasification temperatures of 680 and 780 °C.

the CO_2/CO ratios at gasification temperatures of 680 and 780 °C, and reveals that the homogeneous reaction was dominant at both temperatures. The homogeneous reaction has a relatively much lower activation energy [21] and thus a higher reaction rate. The CO_2/CO ratios at 680 °C were much higher than those at 780 °C, which can be attributed to the tendency of chemical equilibrium. Fig. 6 shows the equilibrium constants of the WGS reaction and S–C reactions at high temperatures of 630–790 °C. The equilibrium constant of the heterogeneous S–C reaction increased rapidly with temperature, whereas that of the homogeneous WGS reaction decreased slightly, strengthening the backward WGS reaction and further decreasing the CO_2 generated and CO consumed in the WGS reaction. However, the equilibrium of the WGS reaction moved toward the reactants, whereas that of the S–C reaction moved toward the products at these high temperatures, eventually causing high CO_2/CO ratios at relatively low gasification temperatures.

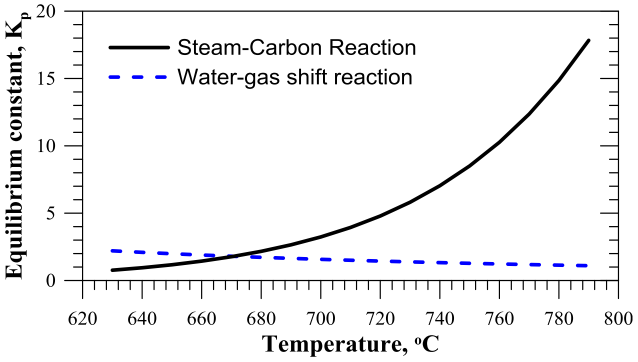

Fig. 6 – Equilibrium constants of WGS and heterogeneous S–C reactions [24,25].

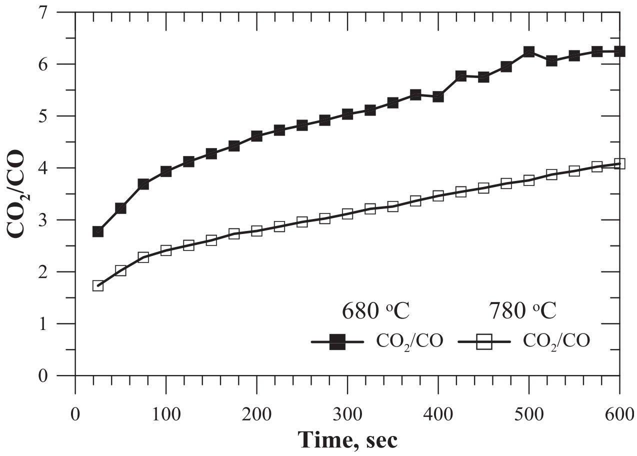

Fig. 5 – Evolution of CO_2/CO ratio at gasification temperatures of 680 and 780 °C.

Effect of nitrogen flow rate

The effect of nitrogen flow rate on hydrogen production was investigated at N_2 flow rates of 0.8 and 1.2 L/min. A low nitrogen flow rate increased the syngas production rate (Fig. 7). The hydrogen production rate at 0.8 L/min was clearly higher than that at 1.2 L/min, and this trend was observed for both CO and CO_2 production rates as well; by contrast, the methane production rates were negligible at these two N_2 flow rates (data not shown). The steam volume fraction in the gasifier decreased with an increase in the nitrogen flow rate, which improved the gasification rate. As shown in Fig. 8, the H_2/CO_2 ratios under these two nitrogen flow rates exceeded 4 in the volatile reaction phase because of methane production, and the H_2/CO_2 ratios approached 2 in the char reaction phase, especially, at a nitrogen flow rate of 1.2 L/min.

The plot of the CO_2/CO ratios at a nitrogen flow rate of 1.2 L/min (Fig. 9) clarifies the effect of the gasifying agent on the homogeneous and heterogeneous gasification reactions. The CO_2/CO ratios exceeded unity, meaning that the reduction in the steam volume fraction in the gasifier affects the heterogeneous S–C reaction more than it does the homogeneous WGS reaction.

Effect of torrefaction temperature

The effect of torrefaction temperature on hydrogen production was investigated using biomass torrefied at 300 °C

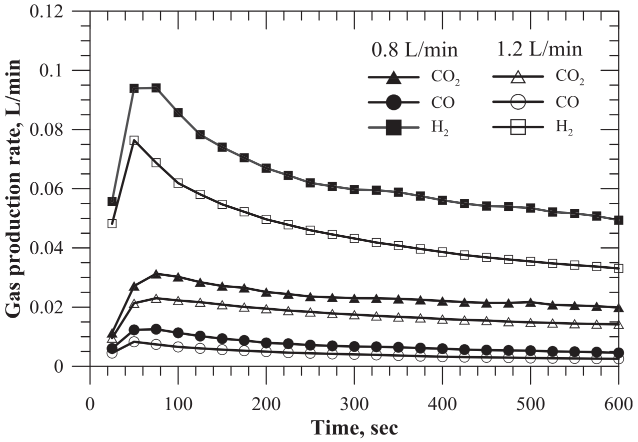

Fig. 7 – Evolution of biosyngas (excluding CH_4) production rate at nitrogen flow rates of 0.8 and 1.2 L/min.

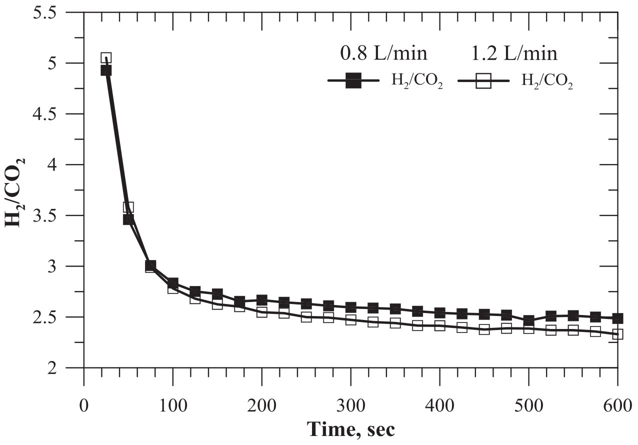

Fig. 8 – Evolution of H_2/CO_2 ratios at nitrogen flow rates of 0.8 and 1.2 L/min.

and raw biomass. The production rate of the main biosyngas was lower when using torrefied biomass than when using raw biomass, and the H_2 and CO_2 production rates were larger when using raw biomass than when using torrefied biomass, as shown in Fig. 10. However, the CO production rates were identical in both cases. Torrefaction pretreatment decreased the biomass mass available for gasification, resulting in a low biosyngas yield. This is because that torrefaction pretreatment removes some of the volatile gas in the biomass, as evidenced by the lower methane production in Fig. 11.

Torrefied biomass is more reactive because of its cracked surface and porous interior structure, as evidenced by the relatively lower CO_2/CO ratio in Fig. 12, which indicates that the heterogeneous S–C reaction was dominant. Despite the substantial difference in the CO_2/CO ratios of the raw and torrefied biomass, the difference in the CO_2/CO ratios at the investigated torrefaction temperatures (250 and 300 °C) was negligible (Fig. 12).

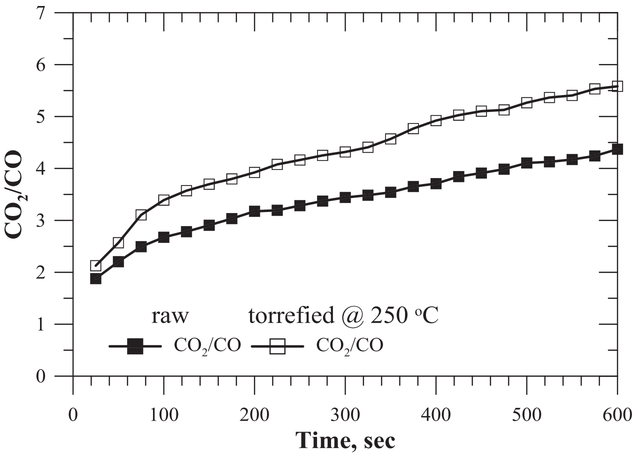

Fig. 9 – Evolution of CO_2/CO ratios at nitrogen flow rates equal of 0.8 and 1.2 L/min.

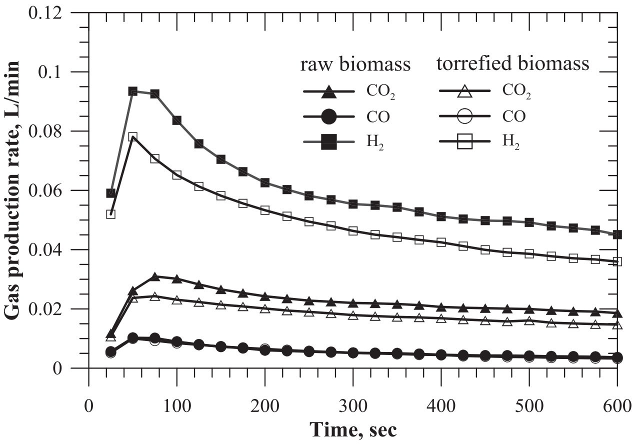

Fig. 10 – Evolution of biosyngas (excluding CH_4) production rate for raw biomass and biomass torrefied at 300 °C.

Effect of steam flow rate

The effect of steam flow rate on hydrogen production was investigated at steam flow rates of 1.2 and 3.0 g/m. Fig. 13 shows the production rates of the main gasification gases (H_2, CO, and CO_2) at these two steam flow rates. The curves of the gas production rates were quite consistent at the investigated flow rates, meaning that the steam flow rate does not significantly affect the production of gases; this result is consistent with Guan et al. [14]. This is because after the necessary steam amount has been supplied, any excessive steam supplied does not influence the gasification reactions. In addition, the H_2/CO_2 ratios did not vary significantly at the two steam flow rates (Fig. 14). Similarly, the strength of the volatile reaction and char reaction phases did not change much with the flow rate. These results indicate that a steam flow rate of 1.2 g/min may be adequate for gasification as the majority of the steam supplied at 3 g/min does not participate in the gasification reactions.

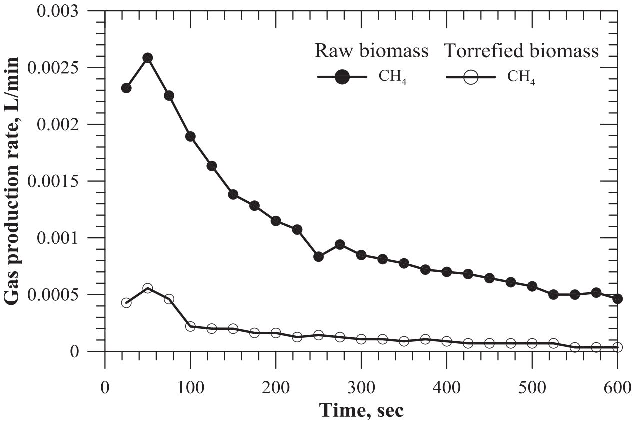

Fig. 11 – Methane production rate for raw biomass and biomass torrefied at 300 °C.

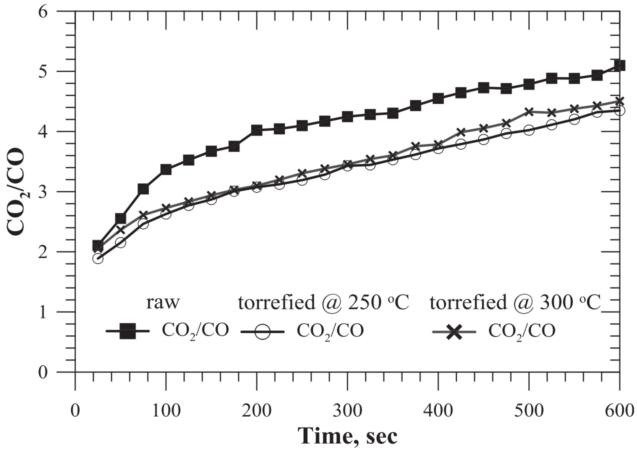

Fig. 12 – CO_2-to-CO ratios under different torrefaction conditions.

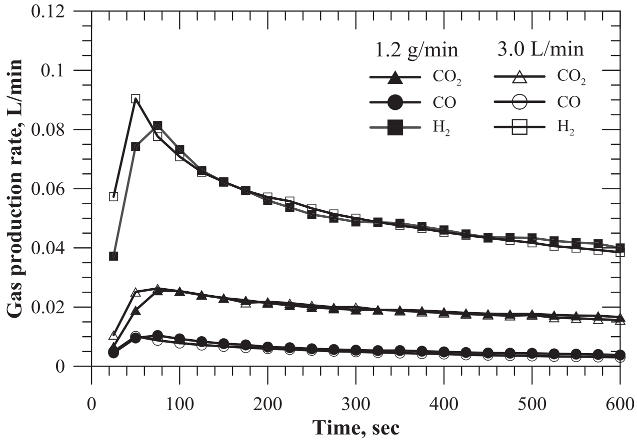

Fig. 13 – Evolution of biosyngas (excluding CH_4) production rate at steam flow rates of 1.2 and 3 g/min.

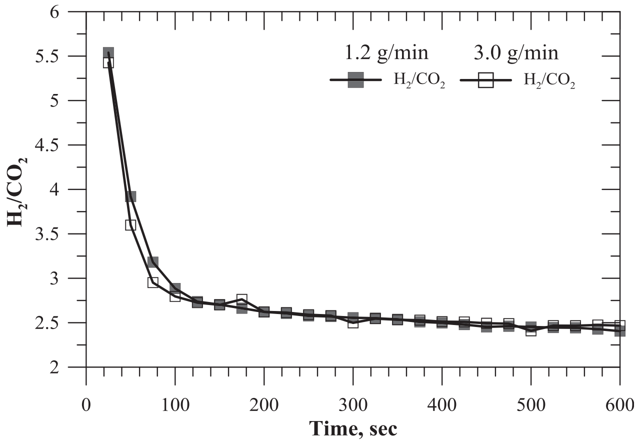

Fig. 14 – Evolution of H_2/CO_2 ratios at steam flow rates of 1.2 and 3 g/min.

Conclusion

The effect of torrefaction pretreatment, gasification temperature, carrier-gas flow rate, and steam flow rate on the yield and composition of syngas during steam gasification was studied. The study conclusions are as follows:

1. The gasification temperature of biomass significantly affects the composition of syngas generated during steam gasification, and the H_2/CO ratio increases by approximately 50% with an increase in temperature ranging from 680 °C to 780 °C. The other investigated factors exhibited weaker effects in the following decreasing order of influence: flow rate > torrefaction temperature > steam flow rate. The higher H_2/CO ratio at a lower gasification temperature increased the energy density of the combustible constituents of the syngas by 3.43%.
2. Methane formation and volatile reactions are dominant in the initial stages of gasification, resulting in a much higher hydrogen concentration and higher H_2/CO_2 ratio in this phase. The subsequent slow char reaction phases have a lower syngas production rate and a lower but nearly constant H_2/CO_2 ratio.
3. A higher temperature and lower nitrogen flow rate increased the yield of syngas by increasing the gasification reaction rate. Torrefaction pretreatment of biomass decreased biomass mass, which decreased the syngas yield.
4. The temperature and torrefaction pretreatment affects the chemical equilibrium in the gasification reaction. Higher temperatures and torrefaction favor the heterogeneous water gas reaction.
5. Steam flow rate does not significantly affect syngas yield and composition.

Acknowledgments

This research was supported by the Ministry of Science and Technology (Republic of China, Taiwan) under Grants MOST 106-2923-E-006-003-MY3 and MOST 106-3113-E-006-002-CC2.

REFERENCES

[1] Williams A, Jones JM, Ma L, Pourkashanian M. Pollutants from the combustion of solid biomass fuels. Prog Energy Combust Sci 2012;38:113–37.
[2] Batidzirai B, Mignot APR, Schakel WB, Junginger HM, Faaij APC. Biomass torrefaction technology: techno-economic status and future prospects. Energy 2013;62:196–214.
[3] Sansaniwal SK, Pal K, Rosen MA, Tyagi SK. Recent advances in the development of biomass gasification technology: a comprehensive review. Renew Sustainable Energy Rev 2017;72:363–84.
[4] Heidenreich S, Foscolo PU. New concepts in biomass gasification. Prog Energy Combust Sci 2015;46:72–95.
[5] Balat H, Kırtay E. Hydrogen from biomass – present scenario and future prospects. Int J Hydrogen Energy 2010;35:7416–26.

[6] de Lasa H, Salaices E, Mazumder J, Lucky R. Catalytic steam gasification of biomass: catalysts, thermodynamics and kinetics. Chem Rev 2011;111:5404–33.

[7] Basu P. Chapter 7-gasification theory, biomass gasification, pyrolysis and torrefaction. 2nd ed. Boston: Academic Press; 2013. p. 199–248.

[8] Chen Q, Zhou J, Liu B, Mei Q, Luo Z. Influence of torrefaction pretreatment on biomass gasification technology. Chin Sci Bull 2011;56:1449–56.

[9] Chew JJ, Doshi V. Recent advances in biomass pretreatment – torrefaction fundamentals and technology. Renew Sustainable Energy Rev 2011;15:4212–22.

[10] Deng J, Wang G-j, Kuang J-h, Zhang Y-l, Luo Y-h. Pretreatment of agricultural residues for co-gasification via torrefaction. J Anal Appl Pyrol 2009;86:331–7.

[11] Prins MJ, Ptasinski KJ, Janssen FJJG. Torrefaction of wood: Part 1. Weight loss kinetics. J Anal Appl Pyrol 2006;77:28–34.

[12] Couhert C, Salvador S, Commandré JM. Impact of torrefaction on syngas production from wood. Fuel 2009;88:2286–90.

[13] Mohammed MAA, Salmiaton A, Wan Azlina WAKG, Mohammad Amran MS, Fakhru'l-Razi A. Air gasification of empty fruit bunch for hydrogen-rich gas production in a fluidized-bed reactor. Energy Convers Manag 2011;52:1555–61.

[14] Kaewpanha M, Guan G, Hao X, Wang Z, Kasai Y, Kusakabe K, et al. Steam co-gasification of brown seaweed and land-based biomass. Fuel Process Technol 2014;120:106–12.

[15] Parthasarathy P, Narayanan KS. Hydrogen production from steam gasification of biomass: influence of process parameters on hydrogen yield – a review. Renew Energy 2014;66:570–9.

[16] Moon J, Lee J, Lee U, Hwang J. Transient behavior of devolatilization and char reaction during steam gasification of biomass. Bioresour Technol 2013;133:429–36.

[17] Sattar A, Leeke GA, Hornung A, Wood J. Steam gasification of rapeseed, wood, sewage sludge and miscanthus biochars for the production of a hydrogen-rich syngas. Biomass Bioenergy 2014;69:276–86.

[18] Chan YH, Dang KV, Yusup S, Lim MT, Zain AM, Uemura Y. Studies on catalytic pyrolysis of empty fruit bunch (EFB) using Taguchi's L9 Orthogonal Array. J Energy Inst 2014;87:227–34.

[19] Chang SH. An overview of empty fruit bunch from oil palm as feedstock for bio-oil production. Biomass Bioenergy 2014;62:174–81.

[20] Gøbel B, Henriksen U, Jensen TK, Qvale B, Houbak N. The development of a computer model for a fixed bed gasifier and its use for optimization and control,. Bioresour Technol 2007;98:2043–52.

[21] Chen C-J, Hung C-I, Chen W-H. Numerical investigation on performance of coal gasification under various injection patterns in an entrained flow gasifier. Appl Energy 2012;100:218–28.

[22] Inayat A, Ahmad MM, Yusup S, Mutalib MIA. Biomass steam gasification with in-situ CO_2 capture for enriched hydrogen gas production: a reaction kinetics modelling approach,. Energies 2010;3:1472.

[23] Wang J, Jiang M, Yao Y, Zhang Y, Cao J. Steam gasification of coal char catalyzed by K_2CO_3 for enhanced production of hydrogen without formation of methane. Fuel 2009;88:1572–9.

[24] Ferrari A, Hunt J, Lita A, Ashley B, Stiegman A. Microwave-specific effects on the equilibrium constants and thermodynamics of the steam–carbon and related reactions. J Phys Chem C 2014;118:9346–56.

[25] Callaghan CA. Kinetics and catalysis of the water-gas-shift reaction: a microkinetic and graph theoretic approach. Naval Undersea Warfare Center; 2006.